Int. J. Heat Mass Transfer. Vol. 35, No. 6, pp. 1545–1555, 1992
Printed in Great Britain

0017–9310/92 $5.00 + 0.00
Pergamon Press Ltd

The forced convective heat transfer from a twisted bundle of insulated electrical conductors in air

V. T. MORGAN†
CSIRO Division of Applied Physics, PO Box 218, Lindfield, NSW 2070, Australia

(*Received* 14 *August* 1990 *and in final form* 28 *June* 1991)

Abstract—An experimental study of the forced convective heat transfer from groups of two, three and four contacting twisted insulated conductors, known as aerial bundled cables, is described. The local surface temperature is very non-uniform. The average Nusselt number/Reynolds number relationship is shown to depend on the choice of the characteristic length. The discontinuity in the Nu/Re curve, which occurs at a critical Reynolds number $Re_{crit} = 5000$ for a single smooth circular cylinder, also occurs with the bundled cables, but at a lower Reynolds number, depending on the number of cores in the cable. For $Re < Re_{crit}$, the Nusselt number of a bundled cable is less than that of a single cylinder, but at $Re > Re_{crit}$, it is greater. The Nusselt number for each cable configuration is given by $Nu = C\,Re^m$, and values of C and m are tabulated for various ranges of Re from 800 to 4×10^4.

INTRODUCTION

TWISTED bundles of insulated conductors (cables) are used extensively for overhead electric power distribution in Europe, North and South America and Australia, particularly where the proximity of buildings and trees causes problems with the use of bare conductors. Although the continued use of such aerial bundled cables (ABC) appears to be assured, there is uncertainty about their current-carrying capacities. This uncertainty stems from inadequate knowledge of the heat transfer from such cables with forced convection. Although the literature contains many studies of the forced convective heat transfer from groups, or banks, of parallel cylinders with various spacings, there appears to be no study of the forced convective heat transfer from contacting parallel cylinders, or contacting twisted cylinders, in crossflow.

This paper describes a wind tunnel study of the convective heat transfer from typical bundled cables used in Australia [1, 2]. The configurations cover the range of two, three and four contacting twisted cylinders.

EXPERIMENTAL WORK

The 7 ft. × 5 ft. (2.13 m × 1.52 m) closed-circuit wind tunnel at the Aeronautical Department of the University of Sydney was used for these tests. The velocity profile across the width of the tunnel was uniform to within ± 1% at 0.8 m s^{-1}. The wind speed was stable at each setting for a long period, and the temperature of the air within the tunnel varied by less than 0.1°C during each heating and cooling cycle of each cable. The intensity of turbulence, measured with a hot-wire anemometer, was 0.1% at 8 m s^{-1}.

A length of each bundled cable in turn was tensioned horizontally across the width of the tunnel at mid-height. Current was supplied to each conductor connected in series from a 240/5 V isolating transformer fed from a Variac to regulate the 240 V 50 Hz supply; and the current, I, was measured by means of a 4000/5 A current transformer, see Fig. 1. The resistance $R_j(T)$ per unit length of each conductor was derived from the magnitude V_j and phase shift Φ_j of the potential difference across a 1 m length of each conductor within the wind tunnel

$$R_j(T) = V_j \cos \phi_j / I_j. \quad (1)$$

A preliminary investigation, using an infra-red imaging system, ascertained that thermocouples with

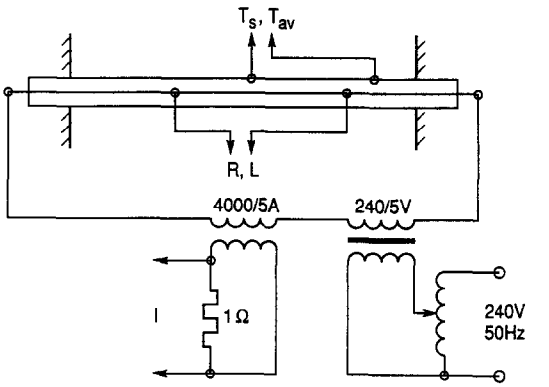

FIG. 1. Circuit for wind-tunnel tests.

† Hooker Visiting Professor, Electrical and Computer Engineering, Department, McMaster University, Hamilton, Ontario, Canada.

NOMENCLATURE

A	total cross-sectional area [m^2]
C	coefficient
D	diameter [m]
F	total perimeter of cable [m]
h	heat transfer coefficient [$W m^{-2} K^{-1}$]
I	current [A]
m	exponent
n	number of cores in cable
Nu	Nusselt number
P	power per unit length [$W m^{-1}$]
R	resistance per unit length [Ωm^{-1}]
Re	Reynolds number
S	surface area per unit length [m]
T	temperature [°C]
T_f	film temperature, $0.5(T_s+T_a)$ [°C]
U	flow velocity [$m s^{-1}$].

Greek symbols

α	temperature coefficient of resistance [K^{-1}]
ε	emissivity
λ	thermal conductivity [$W m^{-1} K^{-1}$]
ν	kinematic viscosity [$m^2 s^{-1}$]
σ	Stefan–Boltzmann constant. $5.6697\times10^{-8} W m^{-2} K^{-4}$.

Subscripts

a	ambient
con	convection
e	effective
f	film
H	hydraulic diameter
J	Joule heating
R	radiation
s	surface of insulation
X	taut string
Y	total exposed area
Z	circumscribing circle.

76 μm, or less, diameter copper and constantan wires were required to ensure that the temperature of the surface of the insulation of the cores could be measured with negligible error due to the conduction of heat along the wires.

An array of 76 μm diameter copper–constantan thermocouples was fitted to the surface of the insulation of each core of the cable at the mid-span position. The temperatures of the surface and the radial centre of each conductor were measured with 300 μm diameter copper–constantan thermocouples, because the 76 μm diameter thermocouples were too fragile to mount in the interior of the cable. A further similar array of thermocouples was mounted on, and within, the cable 30 cm from one wall of the tunnel, to ensure that there was insignificant axial heat conduction to, or from, the external cable and the connecting clamps, which were cooled with fans. The locations of the thermocouples at the midspan position are shown in Fig. 2.

The thermocouples were connected to a multiplexer in a data logger, using an isothermal block. The voltages were measured with a digital voltmeter every minute from the instant of switching on the current until temperature equilibrium had been reached. The temperatures were derived from an algorithm in the memory of a computer, and the results were stored on magnetic disks.

The total power gain per unit length within each cable is given by

$$P_j = \sum_{j=1}^{n} I_j^2 R_j(T) \qquad (2)$$

where

$$\sum_{j=1}^{n} I_j = I.$$

In service, the individual conductor currents may not be exactly equal in magnitude, and are not in phase with each other.

To confirm the resistances $R_j(T)$ measured during the wind-tunnel tests, the cables were dismantled after the tests and the resistance of each conductor was

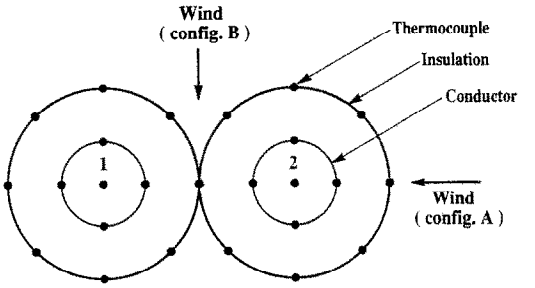

FIG. 2(a).

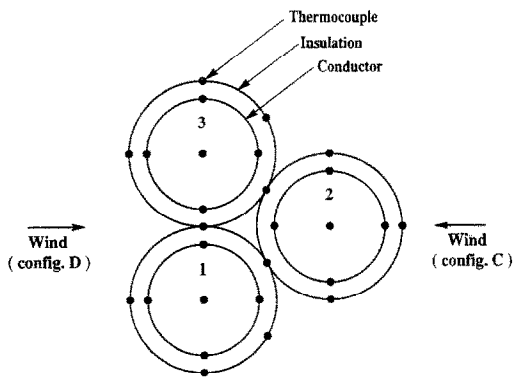

FIG. 2(b).

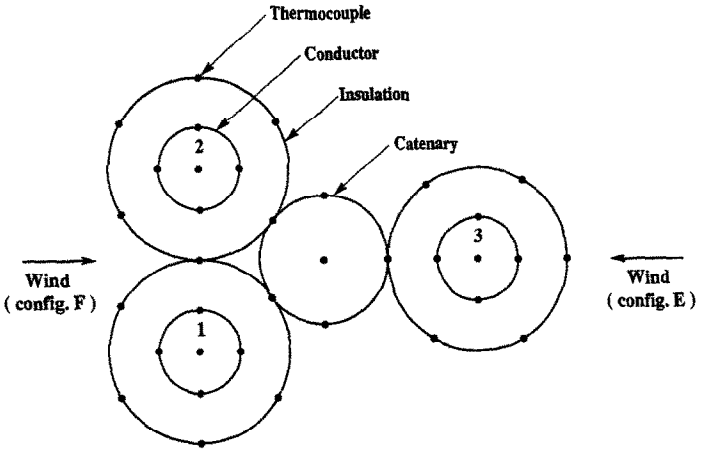

FIG. 2(c).

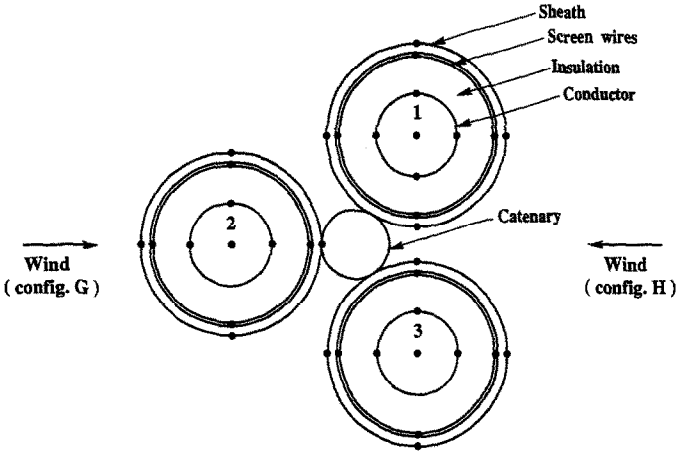

FIG. 2(d).

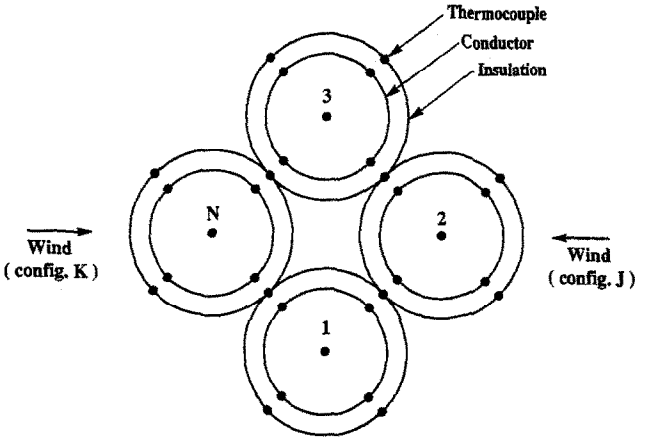

FIG. 2(e).

FIG. 2. Location of thermocouples and configuration with respect to the flow: (a) two-core 35 mm^2 cable; (b) three-core 95 mm^2 cable; (c) three-core 35 mm^2 cable with catenary; (d) three-core 120 mm^2 cable with catenary; (e) four-core 95 mm^2 cable (N = neutral conductor).

measured at 20°C. The resistance at temperature T is

$$R_j(T) = R_j(20)(1+\alpha_{20}(T_{avj}-20)) \quad (3)$$

where $R_j(20)$ is the measured a.c. resistance per unit length of each conductor at 20°C, α_{20} the temperature coefficient of resistance at 20°C, and T_{avj} the mean temperature of conductor j. Skin and proximity effects were negligible.

The power loss per unit length due to radiation from the surface of the insulation is given by

$$P_R = \sum_{j=1}^{n} \varepsilon\sigma S_j((T_{sj}+273)^4-(T_a+273)^4) \quad (4)$$

where ε is the emissivity of the surface, σ the Stefan–Boltzmann constant, S_j the exposed surface area per unit length of core j, T_{sj} the surface temperature of core j, and T_a the ambient temperature. The measured emissivity was $\varepsilon = 0.96$.

The total power loss per unit length due to convection is found from

$$P_{con} = P_J - P_R. \quad (5)$$

Since the Rayleigh number for the measurements varied from 7.8×10^4 to 1.7×10^6, the natural convection had less than 5% effect on the forced convective heat transfer [3].

The overall (average) forced convective heat transfer coefficient is given by

$$h_{con} = P_{con}\Big/\sum_{j=1}^{n} S_j(T_{sj}-T_a) \quad (6)$$

and the Nusselt number is obtained from

$$Nu = h_{con}D_e/\lambda_f \quad (7)$$

and

$$D_e = \sum_{j=1}^{n} S_j/\pi \quad (8)$$

where D_e is the effective diameter of the cable, and λ_f the thermal conductivity of air at the film temperature T_f, given by

$$T_f = 0.5(T_{se}+T_a) \quad (9)$$

where T_{se}, the effective surface temperature, is found from

$$T_{se} = \sum_{j=1}^{n} S_jT_{sj}\Big/\sum_{j=1}^{n} S_j. \quad (10)$$

The Reynolds number is found from

$$Re = UD_e/\nu_f \quad (11)$$

where U is the flow velocity and ν_f the kinematic velocity of air at the film temperature.

There are at least four methods for defining the effective diameter D_e.

(1) *The taut-string method*

This is based on the length of a string transverse to the axis of the cable and stretched around the cores of the cable, see Fig. 3(a). The surface area per unit length is S_X.

(2) *The total-exposed-area method*

This is based on the total exposed area per unit length, see Fig. 3(b)

$$S_Y = \sum_{j=1}^{n} S_j. \quad (12)$$

(3) *The circumscribing-circle method*

This is based on the surface area per unit length S_Z of a cylinder tangential to the surface of the cores of the cable, see Fig. 3(c).

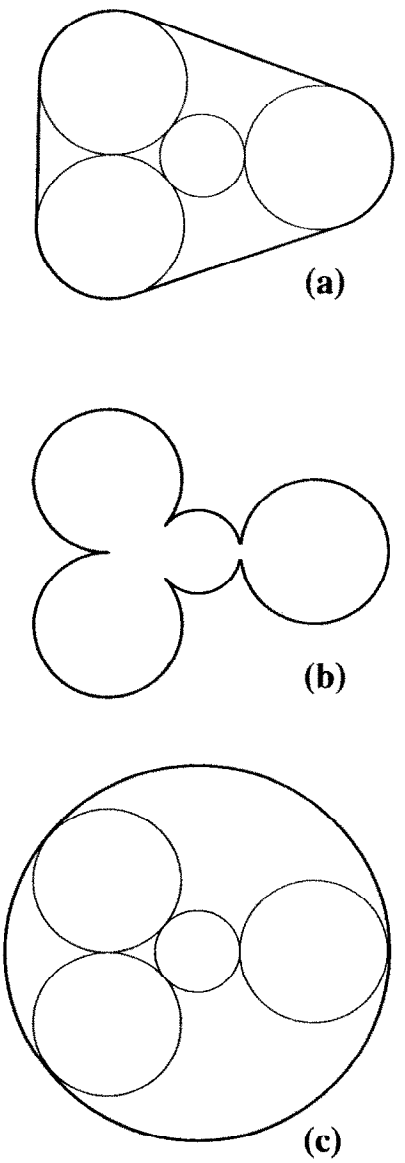

FIG. 3. Effective surface areas for a three-core cable with a catenary: (a) taut string (method X); (b) total exposed surface (method Y); (c) circumscribing circle (method Z).

(4) *The hydraulic diameter method*

The hydraulic diameter is defined as $D_e(H) = 4A/F$, where A is the total cross-sectional area, including air voids, and F the total exposed perimeter of the cable.

The effective diameter of the cable is then obtained from

$$D_e = \frac{S_X}{\pi} \text{ or } \frac{S_Y}{\pi} \text{ or } \frac{S_Z}{\pi} \text{ or } \frac{4A}{F}. \quad (13)$$

Since each core of the cable rotates through 360° relative to the flow direction over an axial distance of one lay length, the task of measuring the overall convective heat transfer for all configurations of each cable was judged to be too onerous, in view of the long heating and cooling cycle times of up to 5 h. Hence, it was decided to study only two configurations: those giving rise to the highest and lowest surface temperatures for the hottest conductor in the cable. The limiting temperature in service is that of the surface of the hottest conductor: it is usually required that this temperature should not exceed 90°C, in order to prevent mechanical degradation of the insulation.

DESCRIPTION OF THE CABLES

Five different cable types were studied, see Fig. 2.

(1) *Two-core* 35 mm^2 *medium-voltage cable* (*Fig.* 2(a))

Conductors. Seven 2.52 mm compacted hard-drawn aluminium strands; overall diameter, 6.95 mm. Resistances at 20°C and 50 Hz: No. 1 core, 8.4583×10^{-4} Ω m^{-1}; No. 2 core, 8.4949×10^{-4} Ω m^{-1}. The conductors were covered with a black semi-conductive screen.

Insulation. High-density polyethylene covered with a smooth black semi-conductive screen; overall diameter, 16.9 mm.

Cable. Two identical cores twisted together, with a lay length (pitch) of 0.81 m; overall diameter, 33.8 mm; mass, 0.5614 kg m^{-1}. The effective diameters are: $D_e(X) = 27.65$ mm, $D_e(Y) = 33.79$ mm, $D_e(Z) = 33.79$ mm and $D_e(H) = 16.90$ mm.

(2) *Three-core* 95 mm^2 *low-voltage cable* (*Fig.* 2(b))

Conductors. Nineteen 2.50 mm compacted hard-drawn aluminium strands; overall diameter 11.5 mm. Resistances at 20°C and 50 Hz: No. 1 core, 3.1330×10^{-4} Ω m^{-1}; No. 2 core, 3.1331×10^{-4} Ω m^{-1}; No. 3 core, 3.1235×10^{-4} Ω m^{-1}.

Insulation. Black, ultraviolet stabilized, extruded cross-linked polyethylene (XLPE); carbon content, 2.5%; thickness, 1.7 mm; overall diameter, 14.9 mm.

Cable. Three identical cores twisted together in triplex formation with a lay length of 0.77 m. Identification of cores: one, two or three longitudinal ribs 0.2 mm high and 2 mm apart. Overall diameter, 32.3 mm; mass, 0.975 kg m^{-1}. The effective diameters are: $D_e(X) = 29.27$ mm, $D_e(Y) = 37.43$ mm, $D_e(Z) = 32.26$ mm and $D_e(H) = 18.19$ mm.

(3) *Three-core* 35 mm^2 *medium-voltage cable with catenary* (*Fig.* 2(c))

Conductors. Seven 2.52 mm compacted hard-drawn aluminium strands; overall diameter, 7.0 mm. Resistances at 20°C and 50 Hz; No. 1 core, 7.8693×10^{-4} Ω m^{-1}; No. 2 core, 7.9936×10^{-4} Ω m^{-1}; No. 3 core, 7.9805×10^{-4} Ω m^{-1}. The conductors were covered with a black semi-conductive screen.

Insulation. High-density polyethylene, diameter 19.9 mm; covered with a smooth black semi-conductive screen with the outside diameter 22.2 mm.

Catenary. Six 4.75 mm hard-drawn aluminium-alloy strands plus seven 1.60 mm galvanized steel strands; outside diameter, 14.25 mm. The catenary did not carry current.

Cable. Three identical cores laid up around the catenary with the lay length 1.47 m. Overall diameter, 58.65 mm; mass, 1.67 kg m^{-1}. The effective diameters are: $D_e(X) = 60.34$ mm, $D_e(Y) = 62.15$ mm, $D_e(Z) = 58.65$ mm and $D_e(H) = 23.81$ mm.

(4) *Three-core* 120 mm^2 *medium-voltage cable with catenary* (*Fig.* 2(d))

Conductors. Nineteen 2.98 mm compacted hard-drawn aluminium strands, with overall diameter 11.95 mm and covered with a black semi-conductive screen. Resistances at 20°C and 50 Hz: No. 1 core, 2.4548×10^{-4} Ω m^{-1}; No. 2 core, 2.4856×10^{-4} Ω m^{-1}; No. 3 core, 2.4891×10^{-4} Ω m^{-1}.

Insulation. XLPE 3.4 mm thick, covered with black semi-conductive screen 0.8 mm thick.

Screen. Thirty nine 1.35 mm copper wires; overall diameter, 26 mm.

Sheath. Smooth black high-density polyethylene 1.8 mm thick; overall diameter, 31.14 mm.

Catenary. Nineteen 2.00 mm bare galvanized steel strands; overall diameter, 10.12 mm. The catenary did not carry current.

Cable. Three identical cores laid up around the catenary, with the lay length 1.74 m. Overall diameter, 72.4 mm; mass, 4.61 kg m^{-1}. The effective diameters are: $D_e(X) = 65.26$ mm, $D_e(Y) = 79.31$ mm, $D_e(Z) = 72.40$ mm and $D_e(H) = 38.48$ mm.

(5) *Four-core* 95 mm^2 *low-voltage cable* (*Fig.* 2(e))

Conductors. Nineteen 2.50 mm compacted hard-drawn aluminium strands with overall diameter 11.5 mm. Resistances at 20°C and 50 Hz: No. 1 core, 3.0785×10^{-4} Ω m^{-1}; No. 2 core, 3.0308×10^{-4} Ω m^{-1}; No. 3 core, 3.0657×10^{-4} Ω m^{-1}. Core No. 4 is the neutral conductor, which normally carries negligible current.

Insulation. Black, UV stabilized extruded XLPE with 2.5% carbon and thickness 1.7 mm; overall diameter, 15.00 mm.

Cable. Four identical cores laid up in square formation, with the lay length 0.91 m. Identification of active cores: one, two or three longitudinal ribs 0.2 mm high and 2 mm apart; neutral core, longitudinal V-shaped serrations evenly spaced around the cir-

cumference. Overall diameter, 36.2 mm; mass, 1.35 kg m^{-1}. The effective diameters are: $D_e(X) = 34.89$ mm, $D_e(Y) = 46.06$ mm, $D_e(Z) = 37.05$ mm and $D_e(H) = 21.22$ mm.

EXPERIMENTAL RESULTS

The results are presented in the form of curves of the average Nusselt number, calculated from equation (7) plotted against the Reynolds number, calculated from equation (11). The log–log curves for the five configurations of cable are represented in Figs. 4–8. For each figure, the values based on the four methods for defining the effective diameter of the cable and the two configurations of the cable with respect to the flow, see Fig. 2, are shown. The reference curve for a single smooth cylinder [3–5] is also plotted in each figure.

The Nusselt number vs Reynolds number characteristics for the various configurations are tabulated in Table 1, where

$$Nu = C\,Re^m \tag{14}$$

and the Nusselt and Reynolds numbers are calculated by the four methods: taut string (X), total exposed area (Y), circumscribing circle (Z) and hydraulic diameter (H). The use of three significant figures for C and m does not imply that the accuracy of each characteristic is better than the estimated uncertainties of $\pm 4\%$; it merely serves to define the position of each curve.

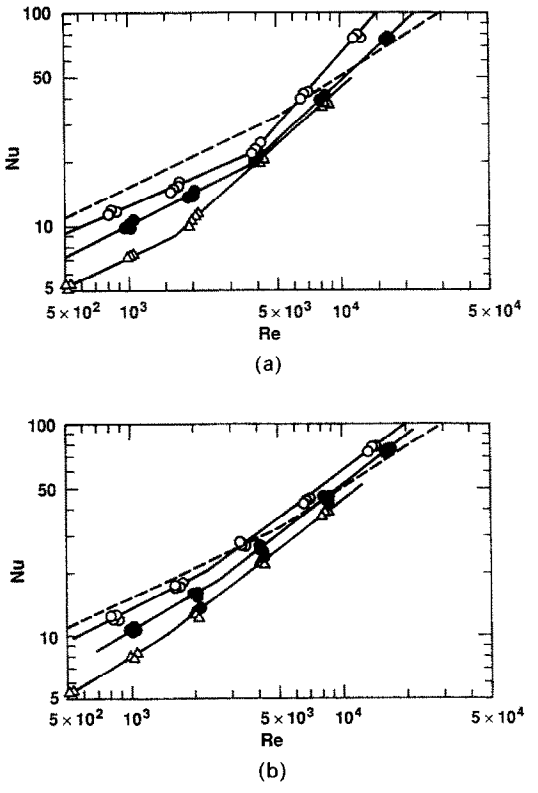

FIG. 4. Two-core 35 mm^2 cable, Nusselt number vs Reynolds number: (a) configuration A; (b) configuration B; ○, method X; ●, methods Y and Z; ———, single smooth cylinder [3, 4]; △, method H.

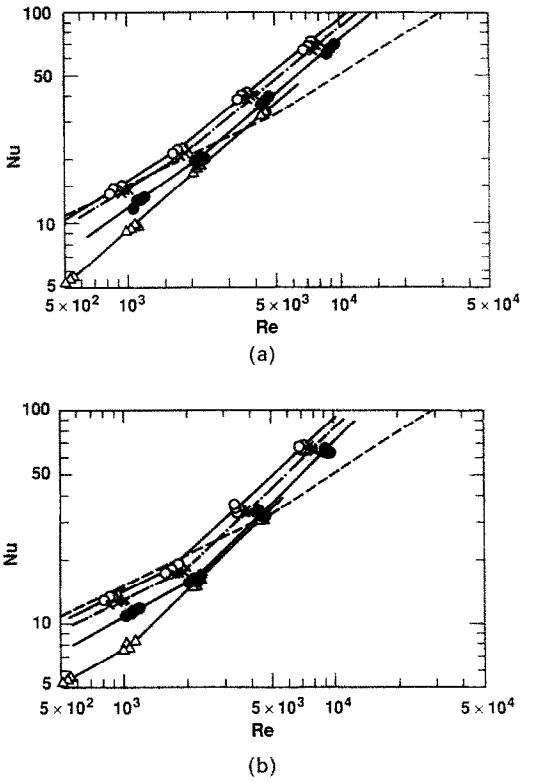

FIG. 5. Three-core 95 mm^2 cable, Nusselt number vs Reynolds number: (a) configuration C; (b) configuration D; ○, method X; ●, method Y; ×, method Z; ———, single smooth cylinder [3, 4]; △, method H.

The temperature distribution around the surface of all the cables was very non-uniform, and varied with the configuration. Since too few thermocouples were installed to obtain a detailed surface distribution of temperature, the relationship $100\,\Delta T_s/\theta_s$ was used as a measure of the non-uniformity, where ΔT_s is the difference between the maximum and minimum local surface temperatures, and θ_s the temperature rise of the mean surface temperature above ambient. This criterion had values in the range 16–65% at $Re = 10^3$, and 43–135% at $Re = 10^4$. The cable having two cores in line had the greatest temperature non-uniformity and the single-core cable had the least non-uniformity.

DISCUSSION

In the case of a single-core cable, it is seen from the dashed curves in Figs. 4–8 that there is a discontinuity in the Nusselt number characteristic at $Re = 5 \times 10^3$ [3–5], which is denoted the critical Reynolds number, Re_{crit}. It is thought that this discontinuity is due to the first eddy in the wake just touching the rear of the

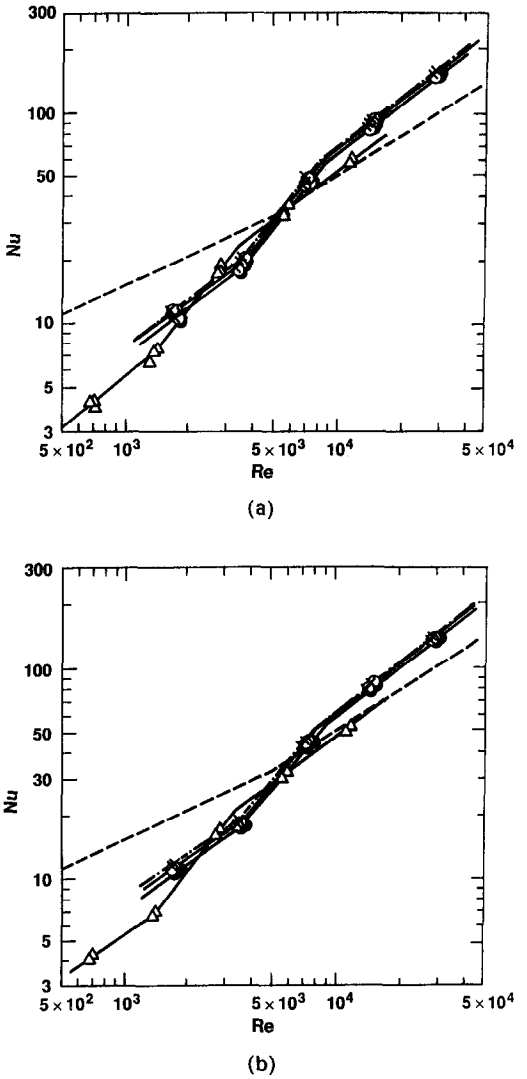

FIG. 6. Three-core 35 mm^2 cable with catenary. Nusselt number vs Reynolds number: (a) configuration E; (b) configuration F; ○, method X; ●, method Y; ×, method Z; ---, single smooth cylinder [3, 4]; △, method H.

cylinder, thus causing an increase in the local heat transfer [4, 6].

It is known that roughness elements on the surface of a cylinder will lower the value of Re_{crit} [7, 8]. Considering bundled cables as rough cylinders, one would anticipate that there would be discontinuities in their Nusselt number vs Reynolds number characteristics at Reynolds numbers less than 5×10^3. That this is the case is confirmed by the results in Figs. 4–8 and Table 1, where it is seen that, for two cores in line (configuration A), $Re_{crit} = 3900$; for two cores side by side (configuration B), $Re_{crit} = 2200$; for three cores (configurations C and D), $Re_{crit} = 1700$–2200; for three 35 mm^2 cores with a catenary (configurations E and F), $Re_{crit} \simeq 3500$; for three 120 mm^2 cores with a catenary, $Re_{crit} = 4000$ (configuration G) or < 1900 (configuration H); and for four cores, $Re_{crit} = 3000$ (configuration K) or 4500 (configuration J).

The lower the critical Reynolds number, the greater will be the convective heat transfer for Reynolds numbers greater than the critical value. Thus, for example, it may be seen from Fig. 4(a) for two cores in line that, although the Nusselt number is initially lower than that for the single core, as a result of the critical Reynolds number occurring at $Re = 3900$ compared with $Re = 5000$ for the single core, the Nusselt number for the two-core cable rapidly surpasses that for the single core, once the critical Reynolds number is exceeded.

It is clear from comparing Fig. 4(a) with Fig. 4(b), etc., that there are differences in the Nusselt number vs Reynolds number characteristics for the various cables, depending on the orientation of the bundle with respect to the direction of flow. However, the mean of the Nusselt numbers for the two configurations studied should approximate to the average Nusselt number for the bundle as it rotates through

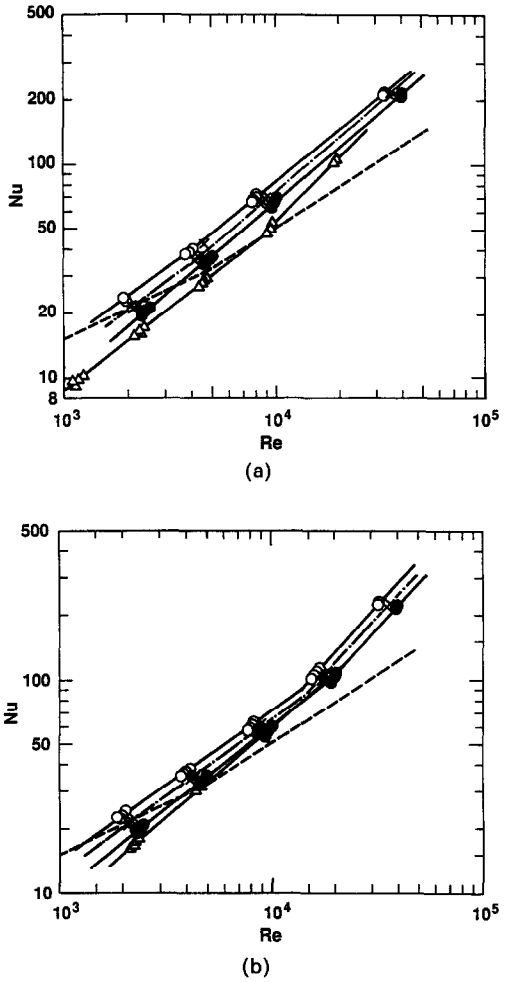

FIG. 7. Three-core 120 mm^2 cable with catenary. Nusselt number vs Reynolds number: (a) configuration G; (b) configuration H; ○, method X; ●, method Y; ×, method Z; ---, single smooth cylinder [3, 4]; △, method H.

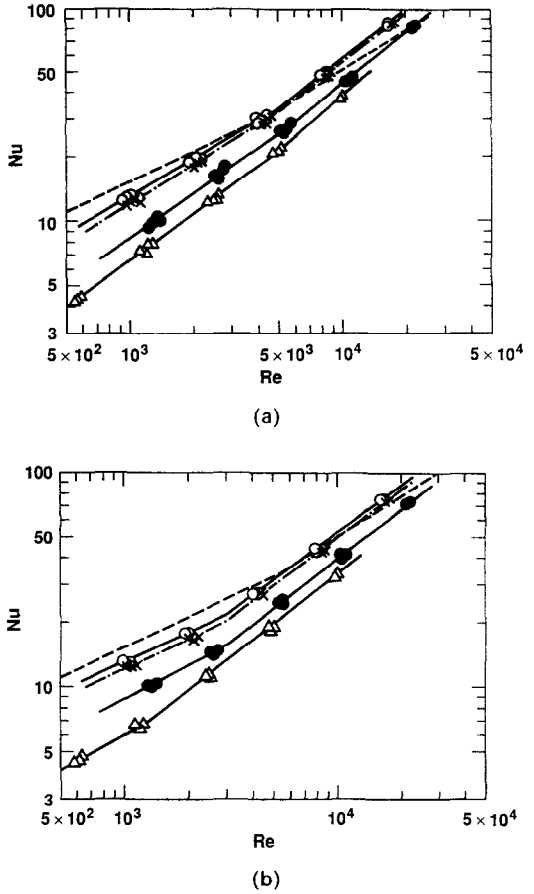

FIG. 8. Four-core 95 mm² cable, Nusselt number vs Reynolds number: (a) configuration J; (b) configuration K; ○, method X; ●, method Y; ×, method Z; ---, single smooth cylinder [3, 4]; △, method H.

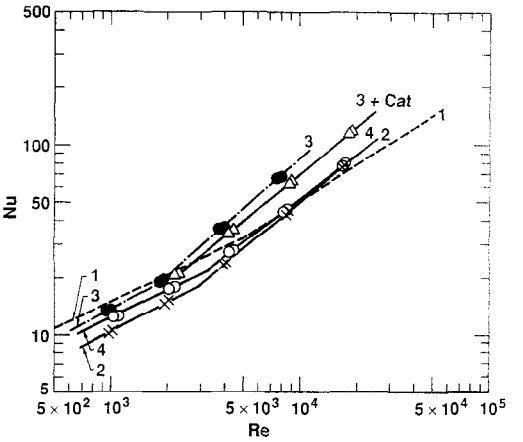

FIG. 9. Mean Nusselt number vs Reynolds number for each type of cable (calculated by method Z): ---, single smooth cylinder [3, 4]; ×, two-core 35 mm² cable; ●, three-core 95 mm² cable; ○, four-core 95 mm² cable; △, three-core 120 mm² cable with catenary.

360° in moving along one lay length (pitch). These mean values are calculated using the circumscribing-circle method (method Z), and are plotted in Fig. 9, where it can be seen that, for $Re < Re_{crit}$, the Nusselt numbers for the two-, three- and four-core cables are less than those for single core, although the curves are parallel with that for the single core. The reductions in Nusselt number for equal Reynolds number are approximately 30% for the two-core cable, 10% for the three-core cable, and 20% for the four-core cable. On the other hand, when $Re > Re_{crit}$, the Nusselt numbers for the bundled cables increase at a greater

Table 1. Heat transfer coefficients

Configuration	Method	Range of Re From	Range of Re To	C	m
A	X	8.0×10^2	3.8×10^3	0.650	0.427
(Figs. 2(a) and 4(a))		3.8×10^3	1.2×10^4	0.00205	1.12
	Y	1.0×10^3	3.9×10^3	0.338	0.491
		3.9×10^3	1.7×10^4	0.00977	0.922
	Z	1.0×10^3	3.9×10^3	0.338	0.491
		3.9×10^3	1.7×10^4	0.00977	0.922
	H	5.0×10^2	1.7×10^3	0.291	0.463
		1.7×10^3	8.6×10^3	0.0120	0.892
B	X	8.0×10^2	2.3×10^3	0.399	0.508
(Figs. 2(a) and 4(b))		2.3×10^3	1.5×10^4	0.0684	0.736
	Y	1.0×10^3	2.2×10^3	0.184	0.585
		2.2×10^3	1.8×10^4	0.0452	0.763
	Z	1.0×10^3	2.2×10^3	0.184	0.585
		2.2×10^3	1.8×10^4	0.0452	0.763
	H	5.0×10^2	1.5×10^3	0.117	0.610
		1.5×10^3	8.6×10^3	0.0383	0.763
C	X	8.0×10^2	1.7×10^3	0.223	0.615
(Figs. 2(b) and 5(a))		1.7×10^3	7.4×10^3	0.0504	0.815
	Y	1.1×10^3	2.2×10^3	0.111	0.674
		2.2×10^3	9.5×10^3	0.0286	0.852
	Z	9.4×10^2	1.9×10^3	0.261	0.583
		1.9×10^3	8.2×10^3	0.0435	0.822
	H	5.0×10^2	4.6×10^3	0.0281	0.840

Table 1.—*Continued*

Configuration	Method	Range of *Re*		C	m
		From	To		
D	X	8.0×10^{2}	1.7×10^{3}	0.517	0.480
(Figs. 2(b) and 5(b))		1.7×10^{3}	7.4×10^{3}	0.0238	0.895
	Y	1.0×10^{3}	2.1×10^{3}	0.261	0.538
		2.1×10^{3}	9.6×10^{3}	0.00972	0.895
	Z	8.5×10^{2}	2.0×10^{3}	0.466	0.480
		2.0×10^{3}	8.0×10^{3}	0.0148	0.936
	H	5.0×10^{2}	1.1×10^{3}	0.157	0.563
		1.1×10^{3}	4.6×10^{3}	0.0101	0.957
E	X	1.9×10^{3}	3.5×10^{3}	0.0474	0.734
(Figs. 2(c) and 6(a))		3.5×10^{3}	8.5×10^{3}	0.000547	1.28
		8.5×10^{3}	3.0×10^{4}	0.0527	0.776
	Y	1.8×10^{3}	3.5×10^{3}	0.0340	0.770
		3.5×10^{3}	8.8×10^{3}	0.000513	1.28
		8.8×10^{3}	3.1×10^{4}	0.0482	0.781
	Z	1.7×10^{3}	3.6×10^{3}	0.0359	0.775
		3.6×10^{3}	8.4×10^{3}	0.0687	1.26
		8.4×10^{3}	2.9×10^{4}	0.0499	0.786
	H	6.8×10^{2}	1.5×10^{3}	0.0182	0.829
		1.5×10^{3}	3.1×10^{3}	0.000640	1.29
		3.1×10^{3}	1.2×10^{4}	0.0525	0.750
F	X	1.7×10^{3}	3.6×10^{3}	0.0684	0.683
(Figs. 2(c) and 6(b))		3.6×10^{3}	8.2×10^{3}	0.000505	1.28
		8.2×10^{3}	3.0×10^{4}	0.0519	0.768
	Y	1.8×10^{3}	3.6×10^{3}	0.0569	0.699
		3.6×10^{3}	9.0×10^{3}	0.000671	1.24
		9.0×10^{3}	3.1×10^{4}	0.0479	0.771
	Z	1.7×10^{3}	3.4×10^{3}	0.0818	0.666
		3.4×10^{3}	8.0×10^{3}	0.000818	1.23
		8.0×10^{3}	2.8×10^{4}	0.0436	0.786
	H	6.8×10^{2}	1.4×10^{3}	0.0452	0.689
		1.4×10^{3}	3.5×10^{3}	0.000578	1.29
		3.5×10^{3}	1.2×10^{4}	0.0522	0.739
G	X	1.9×10^{3}	4.0×10^{3}	0.104	0.717
(Figs. 2(d) and 7(a))		4.0×10^{3}	3.3×10^{4}	0.0510	0.802
	Y	2.4×10^{3}	4.0×10^{4}	0.0278	0.844
	Z	2.1×10^{3}	4.5×10^{3}	0.0732	0.742
		4.5×10^{3}	3.6×10^{4}	0.0314	0.843
	H	1.1×10^{3}	8.0×10^{3}	0.0425	0.765
		8.0×10^{3}	2.0×10^{4}	0.00632	0.980
H	X	1.9×10^{3}	1.4×10^{4}	0.110	0.704
(Figs. 2(d) and 7(b))		1.4×10^{4}	3.3×10^{4}	0.0316	1.08
	Y	2.2×10^{3}	2.0×10^{4}	0.0461	0.779
		2.0×10^{4}	4.0×10^{4}	0.00241	1.08
	Z	2.1×10^{3}	1.5×10^{4}	0.0817	0.725
		1.5×10^{4}	3.7×10^{4}	0.00361	1.05
	H	2.3×10^{3}	2.0×10^{4}	0.0232	0.853
J	X	9.0×10^{2}	4.6×10^{3}	0.227	0.585
(Figs. 2(e) and 8(a))		4.6×10^{3}	1.7×10^{4}	0.0411	0.787
	Y	1.2×10^{3}	5.5×10^{3}	0.0674	0.696
		5.5×10^{3}	2.2×10^{4}	0.0245	0.813
	Z	1.0×10^{3}	4.5×10^{3}	0.182	0.607
		4.5×10^{3}	1.8×10^{4}	0.0409	0.782
	H	5.5×10^{2}	4.7×10^{3}	0.0437	0.725
		4.7×10^{3}	1.0×10^{4}	0.0136	0.863
K	X	9.8×10^{2}	3.1×10^{3}	0.532	0.462
(Figs. 2(e) and 8(b))		3.1×10^{3}	1.7×10^{4}	0.0590	0.736
	Y	1.3×10^{3}	3.0×10^{3}	0.229	0.526
		3.0×10^{3}	2.2×10^{4}	0.0312	0.775
	Z	1.0×10^{3}	3.0×10^{3}	0.464	0.471
		3.0×10^{3}	1.8×10^{4}	0.0499	0.749
	H	5.9×10^{2}	1.8×10^{3}	0.137	0.548
		1.8×10^{3}	1.0×10^{4}	0.0196	0.808

rate than that for the single core. At $Re = 10^4$, these increases are approximately nil for the two-core cable, 70% for the three-core cable, 40% for the three-core cables plus catenary, and 5% for the four-core cable.

A disturbing feature of the results for the multi-core cables is that the Nusselt number vs Reynolds number characteristics differ appreciably when using the four different methods for calculating the effective surface area for convective heat transfer. This raises doubts about which method to use. Traditionally, it has been the practice to use the dimension L_x in the flow direction to categorize the characteristic length of non-circular prisms in calculating Nusselt and Reynolds numbers. In only three of the cable configurations, A, J and K does the effective diameter, calculated from the circumscribing circle (method Z), equal L_x.

Neglecting configurations J and K, which result in rather non-uniform surface temperatures, we can compare in Fig. 4(a) the Nu/Re relationship for the two-core cable having $L_x = D_c$ (filled circles) with that for the single core (dashed line). It is clear that there is a considerable difference between the two characteristics for $Re < Re_{crit}$. It is seen that the characteristic based on the taut-string (method X open circles) results in a better, but not close, agreement between the two curves.

CONCLUSIONS

The following conclusions can be drawn from the results of the wind tunnel study of the heat transfer from aerial bundled cables.

(1) The surface temperature distribution is very non-uniform for all the cable constructions. The least non-uniformity occurs with a single-core cable, and the greatest non-uniformity with a cable having two cores in line.

(2) Different Nusselt number/Reynolds number characteristics are obtained when using different methods for calculating the characteristic length. The taut-string method results in characteristics closest to that for a single circular cylinder, but the agreement is not good.

(3) The discontinuity (kink), which occurs in the Nusselt number/Reynolds number curve for a single smooth circular cylinder at $Re = 5000$, occurs at lower Reynolds numbers for the rougher multi-core bundles. This discontinuity occurs at $Re = 3900$ for two cores in line; at $Re = 2200$ for two cores side by side; at $Re = 1700$–2200 for three cores; at $Re < 1900$ or $Re = 3500$–4000 for three cores plus a catenary, depending on the orientation with respect to the wind; and at $Re = 3000$ or 4500 for four cores.

(4) The lower the Reynolds number at which this discontinuity occurs, the greater is the Nusselt number for Reynolds numbers above the discontinuity.

(5) For Reynolds numbers below the discontinuity, the Nusselt number for the bundled cables is less than that for a single circular cylinder. These reductions in the Nusselt number for equal Reynolds numbers are: 30% for the two-core cable, 10% for the three-core cable, and 20% for the four-core cable.

(6) At $Re = 10^4$, the increase in the Nusselt number above that for a single circular cylinder are: nil for the two-core cable, 70% for the three-core cable, 40% for the three-core cable with a catenary and 5% for the four-core cable.

Acknowledgements—The author gratefully acknowledges the assistance of A. Romijn, who installed the cables in the wind tunnel and fitted the thermocouples; F. J. Berg, who wrote the computer program and supervised the data acquisition; and K. Barber, J. Eisenhuth, N. Pitsis and C. Williamson. The Electricity Supply Association of Australia is thanked for financial support and for permission to publish this paper.

REFERENCES

1. Australian Standard 3560-1988, Electric cables-aerial bundled-voltages up to and including 0.6/1 kV. Standards Association of Australia.
2. Australian Standard 3599.1-1988. Electric cables-aerial bundled-polymeric insulated-voltages 6.35/11(12) kV and 12.7/22(24) kV. Part 1—metallic screened, Standards Association of Australia.
3. V. T. Morgan, The overall convective heat transfer from smooth circular cylinders, *Adv. Heat Transfer* **11**, 199–264 (1975).
4. V. T. Morgan, The forced convective heat transfer from an insulated circular cylindrical conductor in air, *Int. Commun. Heat Mass Transfer* **17**, 367–376 (1990).
5. R. Hilpert, Wärmeabgabe von geheizten Drähten und Rohren in Luftstrom, *Forsch. Geb. IngWes.* **4**, 215–224 (1933).
6. L. Schiller und W. Linke, Druck- und Reibungswiderstand des Zylinders bei Reynoldsschen Zahlen 500 bis 40000, *Z. Flugwiss. Motorluftschiff.* **24**, 193–198 (1933).
7. V. T. Morgan, The heat transfer from bare stranded conductors by natural and forced convection in air, *Int. J. Heat Mass Transfer* **16**, 2023–2034 (1973).
8. R. G. Wylie, Psychrometric wet elements as a basis for precise physico-chemical measurements, *J. Res. Natn. Bur. Stand* **84**, 151–177 (1979).

CONVECTION FORCEE THERMIQUE DANS L'AIR POUR UNE GRAPPE TORSADEE DE CONDUCTEURS ELECTRIQUES ISOLES

Résumé—On étudie expérimentalement la convection forcée thermique pour des groupes de deux, trois et quatre conducteurs isolés torsadés en contact et connus comme cables aériens. La température de la surface est très peu uniforme. La relation entre nombre de Nusselt moyen et nombre de Reynolds dépend du choix de la longueur caractéristique. La discontinuité de la courbe Nu/Re qui apparaît pour un nombre de Reynolds critique $Re_{crit} = 5000$ pour un cylindre unique circulaire et lisse, se produit aussi avec les cables mais pour un nombre de Reynolds plus faible qui dépend du nombre de conducteurs dans le cable. Pour $Re < Re_{crit}$, le nombre de Nusselt d'un cable torsadé est moindre que pour un cylindre unique, mais à $Re > Re_{crit}$ il est supérieur. Le nombre de Nusselt pour la configuration de chaque cable est donnée par $Nu = C\,Re^m$ et les valeurs de C et m sont tabulées pour Re allant de 800 à 4×10^4.

DER WÄRMEÜBERGANG DURCH ERZWUNGENE KONVEKTION AN EINEM VERDRILLTEN BÜNDEL AUS ISOLIERTEN ELEKTRISCHEN LEITERN IN LUFT

Zusammenfassung—Eine experimentelle Untersuchung des Wärmeübergangs durch erzwungene Konvektion an Gruppen aus 2, 3 oder 4 sich berührenden verdrillten isolierten Leitern wird beschrieben. Die örtliche Oberflächentemperatur ist sehr ungleichmäßig. Es zeigt sich, daß die Beziehung zwischen der mittleren Nusselt-Zahl und der Reynolds-Zahl von der Wahl der charakteristischen Abmessung abhängt. Die Unstetigkeit der Nu/Re-Kurve, die bei einem einzelnen glatten Kreiszylinder für eine kritische Reynolds-Zahl $Re_{krit} = 5000$ auftritt, wird bei gebündeltem Kabel ebenfalls beobachtet, jedoch abhängig von der Anzahl der Adern im Bündel bei einer kleineren Reynolds-Zahl. Für $Re < Re_{krit}$ ist die Nusselt-Zahl eines gebündelten Kabels kleiner als diejenige für einen einzelnen Zylinder, für $Re > Re_{krit}$ wird sie jedoch größer. Die Nusselt-Zahl wird für jede Kabelkonfiguration mit Hilfe des Ansatzes $Nu = C\,Re^m$ korreliert; die Werte von C und m sind für verschiedene Bereiche der Reynolds-Zahl zwischen 800 und 4×10^4 tabelliert.

ТЕПЛОПЕРЕНОС ПРИ ВЫНУЖДЕННОЙ КОНВЕКЦИИ ОТ СКРУЧЕННОГО ПУЧКА ИЗОЛИРОВАННЫХ ЭЛЕКТРОПРОВОДОВ В ВОЗДУХЕ

Аннотация—Экспериментально исследуется теплоперенос при вынужденной конвекции от пучков из двух, трех и четырех соприкасающихся скрученных изолированных проводов (воздушного кабеля). Локальная температура поверхности является существенно неоднородной. Показано, что соотношение между числами Нуссельта и Рейнольдса зависит от выбора характерной длины. Разрыв кривой Nu/Re, имеющий место при критическом числе Рейнольдса $Re_{crit} = 5000$ в случае единичного гладкого цилиндра круглого сечения, наблюдается также и в случае кабельных пучков, но при более низком числе Рейнольдса, которое зависит от количества жил кабеля. При $Re < Re_{crit}$ число Нуссельта для кабельного пучка меньше значения для единичного цилиндра, но при $Re > Re_{crit}$ оно превосходит это значение. Для каждой конфигурации кабеля число Нуссельта определяется как $Nu = C\,Re^m$; даются значения C и m для чисел Рейнольдса, изменяющихся от 800 до 4×10^4.